

# Generation of Ultrarelativistic Vortex Leptons with Large Orbital Angular Momenta

Mamutjan Ababekri,<sup>1</sup> Jun-Lin Zhou,<sup>1</sup> Ren-Tong Guo,<sup>1</sup> Yong-Zheng Ren,<sup>1</sup> Yu-Han Kou,<sup>1</sup> Qian Zhao,<sup>1</sup> Zhong-Peng Li,<sup>1</sup> and Jian-Xing Li<sup>1,2,\*</sup>

<sup>1</sup>*Ministry of Education Key Laboratory for Nonequilibrium Synthesis and Modulation of Condensed Matter, Shaanxi Province Key Laboratory of Quantum Information and Quantum Optoelectronic Devices, School of Physics, Xi'an Jiaotong University, Xi'an 710049, China*

<sup>2</sup>*Department of Nuclear Physics, China Institute of Atomic Energy, P. O. Box 275(7), Beijing 102413, China*

(Dated: April 25, 2024)

Ultrarelativistic vortex leptons with intrinsic orbital angular momenta (OAM) have important applications in high energy particle physics, nuclear physics, astrophysics, etc. However, unfortunately, their generation still poses a great challenge. Here, we put forward a novel method for generating ultrarelativistic vortex positrons and electrons through nonlinear Breit-Wheeler (NBW) scattering of vortex  $\gamma$  photons. For the first time, a complete angular momentum-resolved scattering theory has been formulated, introducing the angular momentum of laser photons and vortex particles into the conventional NBW scattering framework. We find that vortex positron (electron) can be produced when the outgoing electron (positron) is generated along the collision axis. By unveiling the angular momentum transfer mechanism, we clarify that OAM of the  $\gamma$  photon and angular momenta of multiple laser photons are entirely transferred to the generated pairs, leading to the production of ultrarelativistic vortex positrons or electrons with large OAM. Furthermore, we find that the cone opening angle and superposition state of the vortex  $\gamma$  photon, distinct characteristics aside from its intrinsic OAM, can be determined via the angular distribution of created pairs in NBW processes. Our method paves the way for investigating strong-field quantum electrodynamics processes concerning the generation and detection of vortex particle beams in intense lasers.

Vortex particles with intrinsic orbital angular momenta (OAM) are characterized by wave packets with helical phase fronts [1–4]. They can introduce novelty to scattering processes owing to their distinctive properties, including large angular momenta (AM) and helical wave fronts, which are absent in conventional spin-polarized particles [5–8]. For example, the collision of ultrarelativistic vortex particle beams presents an opportunity to expand the scope of future colliders [9–11]. The use of ultrarelativistic vortex leptons in deep inelastic scattering experiments has the potential to provide new insights into the spin and OAM constituents of protons, thus offering potential solutions to the long-standing proton spin puzzle [12–15]. Currently, vortex electrons can be produced with kinetic energy up to about 300 keV using spiral phase plates, fork diffraction gratings, or magnetic needles [16–18]. Neutrons and atoms can also be brought into vortex states using similar wavefront engineering techniques at low energies [19–23]. Unfortunately, the generation of ultrarelativistic ones remains a great challenge.

In theory, charged particles can be initially prepared in vortex states at low energies and then accelerated to high energies [24–26]. However, the precise behavior of these particles during high-energy accelerations and the preservation of their vortex structures in practical external fields remain unclear. Another approach to producing high-energy vortex particles involves collision events, utilizing the entanglement of final state particles in scattering processes [27–32]. In this scenario, one final particle can acquire a vortex state if specific post-selection processes are applied to the other final particle. For instance, a generalized measurement can be employed as the post-selection method, measuring the azimuth angle of the

final particle with significant uncertainty to induce the vortex state in the other particle [31]. However, generalized measurement is only known for low energy process [33, 34], and implementing such post-selection on final particles at high energy collisions poses substantial challenges. Another possibility is demonstrated for the Compton scattering process, in which the helical wavefront is transferred from the initial vortex photon to the final vortex  $\gamma$  photon, if the final electron is scattered along the collision axis [27]. Lepton-antilepton pairs can be created through the conversion of light into matter, as demonstrated in the Breit-Wheeler or Bethe-Heitler scattering processes [35–42]. However, the possibility of generating vortex leptons through a feasible post-selection scenario in pair creation dynamics with a substantial probability remains unknown.

Meanwhile, using ultrashort and ultraintense laser pulses [43–47], the nonlinear Breit-Wheeler (NBW) scattering has emerged as a promising method for generating high-brilliance and high-energy positron beams [48–51]. Recent advancements in this field have also revealed the polarization related features of NBW scattering, allowing for the production of polarized pairs [52–60]. However, it is worth noting that current studies primarily focus on investigating the spin angular momentum (SAM) as the only internal degree of freedom [61–68]. Furthermore, since NBW pair creation entails the absorption of multiple laser photons, a substantial amount of AM carried by photons in the laser field is expected to be transferred to the generated pairs. While the overall beam in NBW processes may acquire extrinsic (mechanical) OAM [69–72], the intrinsic OAM carried by scattering particles ( $\gamma$  photons, electrons, and positrons) remain unknown. Nevertheless, the conventional theoretical frameworks of strong-field quantum electrodynamics (SF-QED) for the NBW process have not incorporated the AM of the laser photons and intrinsic OAM of

\* jianxing@xjtu.edu.cn

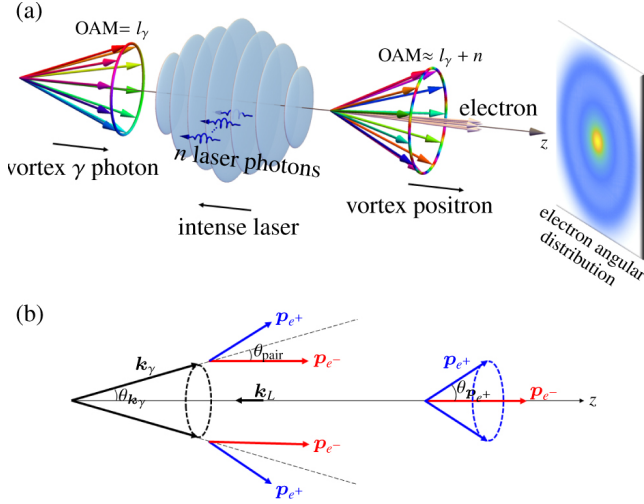


FIG. 1. (a) Generation of ultrarelativistic vortex positron with large OAM via NBW process. A vortex  $\gamma$  photon carrying OAM  $l_\gamma$  collides head-on with a CP laser and absorbs  $n$  laser photons, subsequently decaying into electron and positron pair. When the electron is post-selected along the collision axis, the generated positron assumes a vortex state with OAM  $l_\gamma + n$ . The angular distribution exhibits a bright spot, indicating a maximum probability for electron creation along the collision axis. (b) The condition for producing a vortex positron illustrated in momentum space. The momentum vectors  $\mathbf{k}_\gamma$ ,  $\mathbf{k}_L$ ,  $\mathbf{p}_{e^-}$  and  $\mathbf{p}_{e^+}$  correspond to the  $\gamma$  photon, laser photon, electron and positron, respectively.  $\theta_{k_\gamma}$  is the cone opening angle of the vortex state,  $\theta_{\mathbf{p}_{e^+}}$  is the polar angle of the momentum vector  $\mathbf{p}_{e^+}$ , and  $\theta_{\text{pair}}$  is the NBW pair creation angle relative to the  $\gamma$  photon wave vector  $\mathbf{k}_\gamma$ .

scattering particles [48, 50, 73]. Consequently, the AM transfer mechanism and the formation of a helical wave front in the final state during NBW process are still unclear, leaving the generation of ultrarelativistic vortex leptons in intense lasers an open question.

In this Letter, we investigate the generation of ultrarelativistic vortex positrons and electrons via NBW scattering of a vortex  $\gamma$  photon in a circularly polarized (CP) laser [Fig. 1 (a)]. We first develop the AM-resolved NBW scattering theory within the SF-QED framework [74], incorporating AM of all participating particles: laser photons, vortex  $\gamma$  photon, and the generated leptons. We establish the condition for the vortex positron generation by analyzing kinematic relations in momentum space [Fig. 1 (b)]. When the final electron is produced along the collision axis ( $\mathbf{p}_{e^-} \parallel \hat{z}$ ), the absolute value of the transverse momentum of created positron equals that of incoming vortex  $\gamma$  photon. In this scenario, the positron momentum vector  $\mathbf{p}_{e^+}$  forms a conical structure, indicative of its vortex wave packet. Thus, vortex positrons are generated when the accompanying electrons are post-selected along the collision axis. The normalized probability for electron generation along the axis can reach a maximum (Fig. 2). Under the condition  $\mathbf{p}_{e^-} \parallel \hat{z}$ , we derive the AM conservation relation in Eq. (2) and numerically compute the energy spectra of the vortex positron, and analyze impacts of multiphoton absorption and total SAM from scattering particles (Fig. 3). We find that OAM of the  $\gamma$  photon and AM of multiple laser photons are en-

tirely transferred to the generated vortex positron  $l_{e^+}$ , resulting in  $l_{e^+} \approx l_\gamma + n$ . Therefore, vortex positrons with large OAM can be generated even when the initial  $\gamma$  photon carries small OAM (Fig. 4). These finding also hold for the symmetric case: ultrarelativistic vortex electrons can be generated when the positron is created along the collision axis. Finally, we find the angular distribution of created pairs in NBW scattering can be used to detect the cone opening angle and superposition state of a vortex  $\gamma$  photon (Fig. 5). Throughout, natural units are used ( $\hbar = c = 1$ ), and the fine-structure constant is  $\alpha = \frac{e^2}{4\pi} \approx \frac{1}{137}$ .

The condition for generating vortex positron and electron is determined through the following argument in momentum space [Fig. 1 (b)]. We utilize the Bessel wave function to describe a vortex particle. The momentum vectors  $\mathbf{k}_\gamma$  of the constituent plane waves in such a vortex photon exhibit a conical distribution characterized by an opening angle  $\theta_{k_\gamma}$ , given by  $\theta_{k_\gamma} = \arcsin(|\mathbf{k}_{\gamma,\perp}|/|\mathbf{k}_\gamma|)$ , where  $\mathbf{k}_{\gamma,\perp}$  is the transverse component of the momentum  $\mathbf{k}_\gamma$  [27]. A generated positron can be identified as a Bessel mode vortex particle when it exhibits a similar conical structure in momentum space [75]. For each momentum vector  $\mathbf{k}_\gamma$ , the generated electron-positron pair possesses an angle  $\theta_{\text{pair}}$  with respect to the propagation direction of the plane wave component. Under the condition  $\theta_{\text{pair}} = \theta_{k_\gamma}$ , the plane wave electron is produced along the collision axis, with a zero polar angle with respect to this axis ( $\theta_{\mathbf{p}_{e^-}} = 0$ ), and the momentum vector  $\mathbf{p}_{e^+}$  of the plane wave positron is uniquely determined, exhibiting a fixed polar angle  $\theta_{\mathbf{p}_{e^+}}$ . As the wave vector  $\mathbf{k}_\gamma$  traverses the cone, the momentum  $\mathbf{p}_{e^+}$  of the positron also spreads out over a cone with an opening angle  $\theta_{\mathbf{p}_{e^+}}$ , thereby indicating its vortex state. Note that when electrons are post-selected with a non-zero polar angle  $\theta_{\mathbf{p}_{e^-}} \neq 0$ , corresponding to  $\theta_{\text{pair}} \neq \theta_{k_\gamma}$ , the positron's momentum vector fails to exhibit a conical structure, thereby preventing the positron from adopting a vortex mode. These arguments also apply to the symmetric case. When the positron is created along collision axis ( $\theta_{\mathbf{p}_{e^+}} = 0$ ), the electron momentum  $\mathbf{p}_{e^-}$  lies on a cone, resulting in the generation of a vortex electron. In the following, we continue our exploration of vortex positron generation.

As post-selection of a plane wave electron along collision axis is a crucial condition for vortex positron generation, we analyze the angular distribution of the generated electron. The collision geometry is presented in Fig. 1 (a). The vortex  $\gamma$  photon propagates along the  $z$  axis and collides with an intense laser. The laser is modeled by a CP plane wave field  $A^\mu(\phi = k_L \cdot x) = a g(\phi) \{0, \cos \phi, \sin \phi, 0\}$ , where  $k_L$  denotes the momentum 4-vector of the laser photon,  $a = a_0 m_e / e$  represents the laser intensity, and  $g(\phi)$  denotes the pulse shape function. The vortex  $\gamma$  photon wave function is described by the Bessel wave packet in terms of the plane wave function  $A_\Lambda^\mu(t, \mathbf{r})$  as  $\mathcal{A}_{j,\Lambda}^\mu(t, \mathbf{r}) = \int \frac{d^2 \mathbf{k}_{\gamma,\perp}}{(2\pi)^2} a_{j_\gamma}(\mathbf{k}_{\gamma,\perp}) A_\Lambda^\mu(t, \mathbf{r})$ . Here,  $a_{j_\gamma}(\mathbf{k}_{\gamma,\perp})$  is the vortex amplitude,  $\Lambda$  represents the helicity, and  $j_\gamma$  is the total angular momentum (TAM). The  $S$ -matrix element can be written as  $S_{fi}^{\text{vortex}} = \int \frac{d^2 \mathbf{k}_{\gamma,\perp}}{(2\pi)^2} a_{j_\gamma}(\mathbf{k}_{\gamma,\perp}) S_{fi}^{\text{plane}}$ , with  $S_{fi}^{\text{plane}}$  denoting the usual NBW  $S$ -matrix element for plane wave particles.

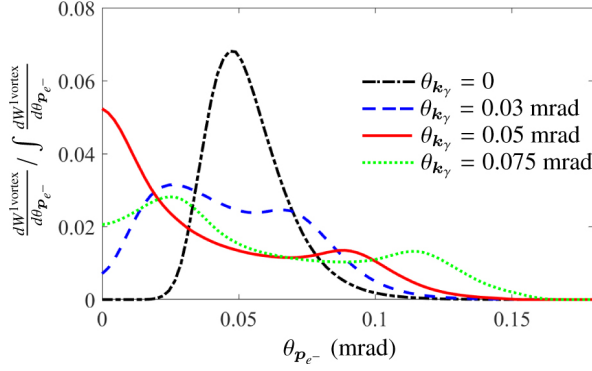


FIG. 2. Normalized probability distribution vs electron's propagation angle  $\theta_{p_{e^-}}$  with respect to the collision axis. The distribution is normalized by the total probability  $\int \frac{dW^{1\text{vortex}}}{d\theta_{p_{e^-}}}$  and presented with the resolution  $\Delta\theta_{p_{e^-}} \approx 0.002$  mrad.  $\theta_{k_\gamma}$  is the vortex  $\gamma$  photon's cone opening angle.  $\theta_{k_\gamma} = 0$  corresponds to the case of plane wave  $\gamma$  photon scattering with the laser along the collision axis.

This leads to the angle-differential probability for the electron

$$\frac{dW^{1\text{vortex}}(\theta_{k_\gamma})}{d\Omega_{e^-}} = \int \frac{d\varphi_{k_\gamma}}{2\pi} F(\varphi_{k_\gamma}) \frac{dW^{\text{plane}}(\theta_{k_\gamma}, \varphi_{k_\gamma})}{d\Omega_{e^-}}, \quad (1)$$

where  $dW^{\text{plane}}(\theta_{k_\gamma}, \varphi_{k_\gamma})/d\Omega_{e^-}$  represents the pair creation rate with a plane wave  $\gamma$  photon. We define  $\theta_{p_{e^-}} = \sqrt{\theta_{e^-x}^2 + \theta_{e^-y}^2}$  by introducing  $d\Omega_{e^-} = d\theta_{e^-x}d\theta_{e^-y}$ . The definition of  $F(\varphi_{k_\gamma})$  and other details on the derivation of Eq. (1) are provided in [74]. We set laser intensity to  $a_0 = 1$  and employ the pulse shape function  $g(\phi) = \sin^2(\frac{\phi}{2N_{\text{cycle}}})$ , where the number of laser pulse cycles is set as  $N_{\text{cycle}} = 8$ , and the central laser frequency is  $\omega_L = 1.55$  eV. The energy of the vortex  $\gamma$  photon is set to  $\varepsilon_\gamma = 20$  GeV, and calculations are conducted for various values of vortex  $\gamma$  photon's cone opening angle  $\theta_{k_\gamma}$  (Fig 2). Corresponding results in the  $\theta_{e^-x}\theta_{e^-y}$  plane are presented in Fig. S1 of [74]. The maximum probability for electron generation along the collision axis ( $\theta_{p_{e^-}} = 0$ ) occurs when the vortex  $\gamma$  photon has a cone opening angle of  $\theta_{k_\gamma} = 0.05$  mrad, as depicted by the solid red line in Fig. 2. In the plane wave limit of the  $\gamma$  photon, where the cone opening angle is zero ( $\theta_{k_\gamma} = 0$ ), the electron predominantly emerges at an angle of  $\theta_{p_{e^-}} = 0.05$  mrad relative to the collision axis, as evidenced by the peak position of the dot-dashed black line in Fig. 2. Therefore, optimizing the probability for electron generation along the collision axis occurs when the cone opening angle of the vortex  $\gamma$  photon aligns with the dominant pair creation angle associated with the plane-wave component of the  $\gamma$  photon. In principle, vortex positron generation is also feasible using  $\gamma$  photons of lower energies. To attain a substantial probability in such scenarios, it is necessary to increase either the laser intensity  $a_0$  or the laser frequency  $\omega_L$ . However, it is crucial to note that employing ultraintense lasers ( $a_0 \gg 1$ ) may initiate cascades involving multiple radiation emissions and pair creations, necessitating careful consideration of these complex events.

We obtain the vortex positron generation probability and

elucidate the AM transfer mechanism by applying the post-selection condition  $\theta_{p_{e^-}} = 0$ . However, the conventional NBW scattering theory is inadequate for investigating the AM conservation relation, as it solely considers the SAM contributions of the scattering particles while disregarding the AM contributions from laser photons and the vortex particles. To address these limitations, we develop an AM-resolved NBW scattering theory [74]. The  $S$ -matrix element describing vortex positron generation can be expressed as  $S_{fi}^{2\text{vortex}} = \int \frac{d^2\mathbf{k}_{\gamma,\perp}}{(2\pi)^2} \frac{d^2\mathbf{p}_{e^+,\perp}}{(2\pi)^2} a_{j_\gamma}(\mathbf{k}_{\gamma,\perp}) a_{j_{e^+}}^*(\mathbf{p}_{e^+,\perp}) S_{fi}^{\text{plane}}$ , where  $a_{j_\gamma}(\mathbf{k}_{\gamma,\perp})$  and  $a_{j_{e^+}}^*(\mathbf{p}_{e^+,\perp})$  represent vortex amplitudes of the  $\gamma$  photon (with TAM  $j_\gamma$ ) and the positron (with TAM  $j_{e^+}$ ), respectively. The vortex state is an eigenfunction of the TAM operator, and under the paraxial approximation, it becomes an eigenfunction of both the OAM and SAM operators [76]. The probability for the generation of vortex positron reads

$$\frac{dW_n^{2\text{vortex}}}{d\varepsilon_{e^+}} = \frac{\alpha}{4\varepsilon_\gamma} \frac{\varepsilon_{e^+} p_{e^+,z}}{(k_L p_{e^-})(k_L p_{e^+})} \delta_{j_\gamma+n, j_{e^+}+s_{e^-}} |\mathcal{M}_n(s)|^2, \quad (2)$$

where the harmonic amplitude  $\mathcal{M}_n(s)$  is defined in [74]. The AM transfer relation can be identified from the AM conserving  $\delta$ -function, which enables one to express the TAM of the created vortex positron as  $j_{e^+} = j_\gamma + n - s_{e^-}$ . Thus, the vortex positron receives AM contributions from the  $\gamma$  photon ( $j_\gamma$ ), the multiple laser photons ( $n$ ), and the SAM of the electron ( $s_{e^-}$ ). Here, laser photons impart extra AM into the scattering process, enhancing the contribution from the vortex  $\gamma$  photon  $j_\gamma$  by  $n$ . Given the substantial number of laser photons required to exceed the energy threshold for pair creation, the vortex positron can acquire a significant AM even when the TAM of the incoming  $\gamma$  photon is small. This characteristic of multiphoton absorption, facilitated by intense lasers, is lacking in linear scattering processes [77, 78].

The energy spectrum of the vortex positron is determined numerically by utilizing Eq. (2). We display the results for a vortex  $\gamma$  photon with an energy of  $\varepsilon_\gamma = 20$  GeV and a cone opening angle of  $\theta_{k_\gamma} = 0.05$  mrad ( $|\mathbf{k}_{\gamma,\perp}| = 1$  MeV), employing the same laser configuration as in Fig. 2. As shown in Fig. 3 (a), the vortex positron is produced with a broad energy spectrum, which is a typical result of NBW process taking place within intense laser pulses. Given the relation  $|\mathbf{p}_{e^+,\perp}| = |\mathbf{k}_{\gamma,\perp}|$ , the energy of the vortex positron,  $\varepsilon_{e^+}$ , and its cone opening angle,  $\theta_{p_{e^+}} = \arcsin |\mathbf{p}_{e^+,\perp}|/|\mathbf{p}_{e^+}|$ , satisfy the approximate relation  $\varepsilon_{e^+} \approx |\mathbf{k}_{\gamma,\perp}|/\theta_{p_{e^+}}$  [the dashed red line in Fig. 3 (a)]. Moreover, considering the kinematic condition  $\theta_{p_{e^-}} = 0$ , specifying the energy  $\varepsilon_{e^+}$  of the positron uniquely determines its polar angle  $\theta_{p_{e^+}}$ , thereby defining a conical shape in momentum space. The remaining aspect to be characterized is its AM property.

Both the AM of absorbed laser photons and the spin contributions from the scattering particles play significant roles in determining the AM of the resulting positron. To investigate these influences, we examine the energy spectra of the generated positrons in relation to the harmonics [Fig.3 (b)], as well as various spin configurations of the scattering particles [Fig.3 (c) and (d)]. The finite pulse shape results in a broad energy spectrum for laser photons, each carrying 1 unit of SAM due to their circular polarization [13]. As a result, different harmonics are expected to contribute to the creation of the positron

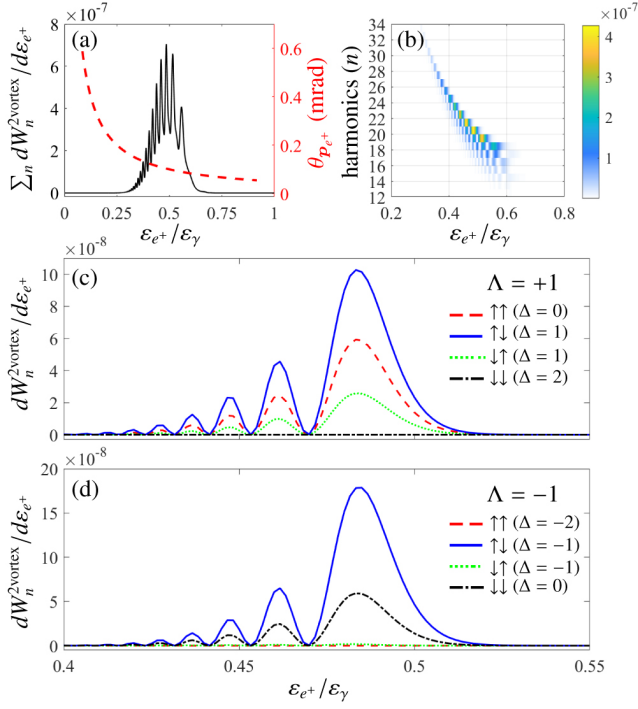


FIG. 3. (a) Solid black line: The probability distribution of the vortex positron generation with respect to the energy ratio  $\varepsilon_{e^+}/\varepsilon_\gamma$ . The probability is summed for NBW harmonics and particle spins. Dashed red line: Vortex positron's cone opening angle  $\theta_{p_{e^+}}$  vs the energy ratio  $\varepsilon_{e^+}/\varepsilon_\gamma$ . (b) The probability distribution of the vortex positron generation with respect to NBW harmonics  $n$  and the energy ratio  $\varepsilon_{e^+}/\varepsilon_\gamma$ . (c) and (d): Probability distributions of the vortex positron generation with respect to the energy ratio  $\varepsilon_{e^+}/\varepsilon_\gamma$  for the fixed harmonic  $n = 20$  for different  $\gamma$  photon helicities  $\Lambda = +1$  and  $\Lambda = -1$ , respectively. The arrows on the left (right) represent the electron (positron) spin states with  $\uparrow$  and  $\downarrow$  denoting  $s_{e^-/e^+} = \frac{1}{2}$  and  $s_{e^-/e^+} = -\frac{1}{2}$ , respectively. The spin contributions from scattering particles are defined as  $\Delta = \Lambda - s_{e^-} - s_{e^+}$ .

with the same energy [Fig. 3 (b)]. Here, the  $n$ th harmonic contributes an AM number of  $n$  to the pair creation event. To determine the OAM number of the vortex positron, we first fix the harmonic number  $n$  and explore the influence of spin effects from other scattering particles. In our collision scenario, with particle energies in the multi-GeV range and transverse momenta below a few MeV, the paraxial approximation holds, rendering the intrinsic spin-orbit-interaction associated with the vortex particle negligible. Consequently, TAM of the vortex particle can be decomposed into SAM and OAM [76]. The OAM of the vortex  $\gamma$  photon is given by  $l_\gamma = j_\gamma - \Lambda$ , while that of the vortex positron is  $l_{e^+} = j_{e^+} - s_{e^+}$ , resulting in the relation  $l_{e^+} = l_\gamma + n + \Delta$  with  $\Delta = \Lambda - s_{e^-} - s_{e^+}$ . Here,  $\Delta$  encapsulates the spin contributions from the scattering particles. To determine  $l_{e^+}$ , one must further identify  $\Delta$ , which assumes integer values within the range  $-2 \leq \Delta \leq 2$ , depending on the SAM of the scattering particles. In Figs. 3 (c) and (d), the pair creation rates for eight distinct spin combinations are depicted, with two of these combinations being significantly suppressed, corresponding to  $\Delta = \pm 2$ . Consequently, the contributing values of

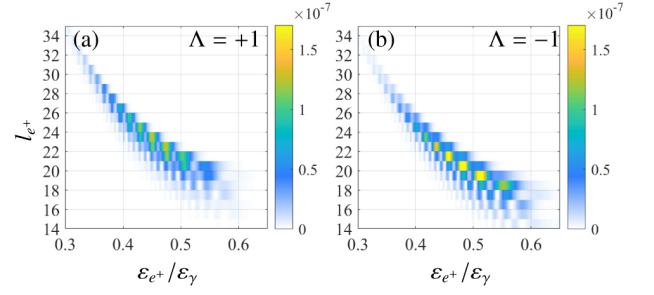


FIG. 4. The probability distribution of the vortex positron generation with respect to positron's OAM and the energy ratio  $\varepsilon_{e^+}/\varepsilon_\gamma$ .  $\gamma$  photon carries OAM  $l_\gamma = 1$  and its helicity takes values (a)  $\Lambda = +1$  and (b)  $\Lambda = -1$ . The same set of  $\gamma$  photon and laser pulse parameters are used as in Fig. 3.

$\Delta$  are limited to  $\{-1, 0, 1\}$ . Given that a substantial number of laser photons ( $n \gg \Delta$ ) participate in the pair creation process, the OAM of the vortex positron arises from transfer of OAM from the initial  $\gamma$  photon and the AM of multiple laser photons, leading to  $l_{e^+} \approx l_\gamma + n$ .

The OAM- and energy-resolved probability distributions for the generated vortex positron are presented in Fig. 4. Considering the relation  $l_{e^+} = l_\gamma + n + \Delta$ , different harmonics  $n$  and distinct combinations of scattering particles' spins ( $\Delta$ ) can yield the same OAM for the vortex positron. Given the specified parameters  $\omega_L = 1.55$  eV and  $\omega = 20$  GeV, it is estimated that the number of absorbed laser photons exceeds  $n \gtrsim 17$ . As a result, even when the initial  $\gamma$  photon has  $l_\gamma = 1$ , the resulting positron attains a substantial OAM (Fig. 4). Upon comparing the results in Figs. 4 (a) and (b), it becomes apparent that the vortex  $\gamma$  photon with negative helicity ( $\Lambda = -1$ ) is more favorable, exhibiting a relatively higher probability than its positive helicity counterpart. Notably, the OAM of the  $\gamma$  photon and AM of the multiple laser photons are transferred solely to the positron, leaving the electron as plane wave particle. This scenario differs from NBW pair creation processes involving extrinsic OAM, where both the electron and positron acquire same amount of AM [69–72].

Considering the experimental feasibility of our proposal, vortex  $\gamma$  photons can be produced via Compton scattering or radiation processes utilizing vortex lasers, CP lasers, or helical undulators [27, 79–82]. The pair creation set up is considered for the multiphoton regime ( $a_0 \gtrsim 1$ ) [83, 84], with  $\gamma$  photon energies typically ranging around  $\varepsilon_\gamma \sim$  GeV to ensure a substantial probability of pair creation in optical lasers. The parameters used in our numerical calculations align with those utilized in the E144 experiment [83] as well as those planned for upcoming experimental setups [85–87]. Beyond their intrinsic OAM, vortex particles exhibit distinctive transverse coherence, manifesting in the form of a cone opening angle. This unique feature is anticipated to introduce novel kinematic aspects to scattering phenomena. In the context of our study, the cone opening angle  $\theta_{k_\gamma}$  of the vortex  $\gamma$  photon plays a pivotal role in optimizing the generation of vortex positrons, as exemplified in Fig. 2. We demonstrate the feasibility of detecting this angle by analyzing the created pairs' angular

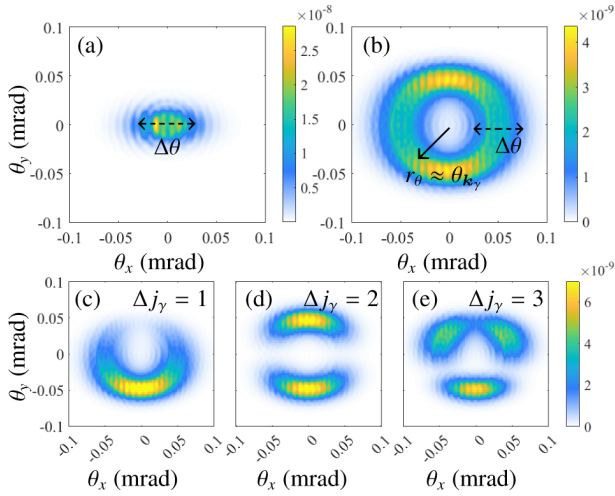


FIG. 5. The probability distribution  $dW^{1\text{vortex}}(\theta_{k_\gamma})/d\Omega_{e^-}$  of the electron with respect to its propagation angle in the  $\theta_{e^-x}\theta_{e^-y}$  plane during NBW scattering of the  $\gamma$  photon in LP lasers. The  $\gamma$  photon is in (a) a plane wave state and (b) a vortex state.  $\gamma$  photons are in the vortex superposition states with  $\Delta j_\gamma = 1$ ,  $\Delta j_\gamma = 2$  and  $\Delta j_\gamma = 3$  in (c), (d) and (e), respectively.

distribution during NBW process. The numerical results are obtained by using Eq. (1) for a linearly polarized laser pulse  $A^\mu(\phi) = a g(\phi) \{0, \cos \phi, 0, 0\}$  with intensity  $a_0 = 1$ , for the same vortex  $\gamma$  photon parameter as in Fig. 3 (results for the CP laser are given in [74]). When the incoming  $\gamma$  photon is in the plane wave state ( $\theta_{k_\gamma} = 0$ ), the created electron is concentrated at the center, exhibiting a diameter  $\Delta\theta$  that corresponds to the full width at half maximum (FWHM) of the electron's angular distribution in the  $\theta_{e^-x}\theta_{e^-y}$  plane [Fig. 5 (a)]. The vortex state of the  $\gamma$  photon causes the angular distribution of the electron to spread along a circle with radius  $r_\theta$  and thickness  $\Delta\theta$  [Fig. 5 (b)].  $r_\theta$  represents the radial distance from the center to the peak position of the probability distribution ring in the  $\theta_{e^-x}\theta_{e^-y}$  plane. We observe that the radius of the electron angle distri-

bution  $r_\theta$  is closely related to the polar angle of the vortex  $\gamma$  photon  $\theta_{k_\gamma} \approx r_\theta$ , thus one can discern the polar angle  $\theta_{k_\gamma}$  by measuring  $r_\theta$ . However, to clearly resolve the polar angle, the process should satisfy  $r_\theta \gtrsim \Delta\theta$ , hence one obtains the condition  $\theta_{k_\gamma} \gtrsim \Delta\theta$ . Estimating  $\Delta\theta \sim a_0 m_e / \varepsilon_\gamma$  [88], the condition for effective measurement poses an upper limit on the laser intensity  $a_0 \lesssim |k_{\gamma,\perp}| / m_e$ . Furthermore, when the vortex  $\gamma$  photon exists in a superposition state, e.g., with two distinct TAM values  $j_{\gamma,1}$  and  $j_{\gamma,2}$ —a scenario possible in the generation of vortex  $\gamma$  photons via nonlinear Compton scattering in pulsed lasers [81]—discrete patterns arise, associated with the difference  $\Delta j_\gamma = j_{\gamma,1} - j_{\gamma,2}$ , which is evident in the function  $F(\varphi_{k_\gamma})$  of Eq. (1) [74]. In this case, the electron angle distribution can still reveal the polar angle  $\theta_{k_\gamma}$ , as pairs are created along the circle with radius  $r_\theta \approx \theta_{k_\gamma}$  [Figs. 5 (c)-(d)].

In conclusion, we put forward a novel method of generating ultrarelativistic vortex positrons and electrons with large OAM through NBW scattering of vortex  $\gamma$  photon in CP lasers. We first develop a complete AM-resolved quantum scattering theory and reveal the OAM-transfer mechanism of NBW process. Our theoretical framework can be further developed to investigate vortex particle generation and detection in other SF-QED processes, and our findings also pave the way for the application of ultrarelativistic vortex leptons in high-energy particle physics, nuclear physics, astrophysics, etc.

*Acknowledgment:* The work is supported by the National Natural Science Foundation of China (Grants No. U2267204, No. 12105217, No. 12147176), the Foundation of Science and Technology on Plasma Physics Laboratory (No. JCKYS2021212008), the Natural Science Basic Research Program of Shaanxi (Grant No. 2023-JC-QN-0091, No. 2024JC-YBQN-0042), and the Shaanxi Fundamental Science Research Project for Mathematics and Physics (Grant No. 22JSY014, No. 22JSQ019).

- 
- [1] L. Allen, M. W. Beijersbergen, and R. Spreeuw *et al.*, Orbital angular momentum of light and the transformation of Laguerre-Gaussian laser modes, *Phys. Rev. A* **45**, 8185 (1992).
  - [2] K. Y. Bliokh, I. P. Ivanov, and G. Guzzinati *et al.*, Theory and applications of free-electron vortex states, *Phys. Rep.* **690**, 1 (2017).
  - [3] S. Lloyd, M. Babiker, G. Thirunavukkarasu, and J. Yuan, Electron vortices: Beams with orbital angular momentum, *Rev. Mod. Phys.* **89**, 035004 (2017).
  - [4] B. A. Knyazev and V. Serbo, Beams of photons with nonzero projections of orbital angular momenta: new results, *Phys. Usp.* **61**, 449 (2018).
  - [5] I. P. Ivanov, N. Korchagin, A. Pimikov, and P. Zhang, Doing spin physics with unpolarized particles, *Phys. Rev. Lett.* **124**, 192001 (2020).
  - [6] D. Budker, M. Gorchtein, and A. Surzhykov *et al.*, Expanding nuclear physics horizons with the Gamma Factory, *Annalen Phys.* **534**, 2100284 (2021).
  - [7] I. P. Ivanov, Promises and challenges of high-energy vortex states collisions, *Prog. Part. Nucl. Phys.* **127**, 103987 (2022).
  - [8] Z.-W. Lu *et al.*, Manipulation of Giant Multipole Resonances via Vortex  $\gamma$  Photons, *Phys. Rev. Lett.* **131**, 202502 (2023).
  - [9] M. Benedikt, A. Blondel, P. Janot, M. Mangano, and F. Zimmermann, Future Circular Colliders succeeding the LHC, *Nature Phys.* **16**, 402 (2020).
  - [10] V. Shiltsev and F. Zimmermann, Modern and Future Colliders, *Rev. Mod. Phys.* **93**, 015006 (2021).
  - [11] D. P. Anderle *et al.*, Electron-ion collider in China, *Front. Phys. (Beijing)* **16**, 64701 (2021).
  - [12] C. A. Aidala, S. D. Bass, D. Hasch, and G. K. Mallot, The Spin Structure of the Nucleon, *Rev. Mod. Phys.* **85**, 655 (2013).
  - [13] E. Leader and C. Lorcé, The angular momentum controversy: What's it all about and does it matter?, *Phys. Rept.* **541**, 163 (2014).

- [14] H. Larocque, I. Kaminer, V. Grillo, R. W. Boyd, and E. Karimi, Twisting neutrons may reveal their internal structure, *Nature Phys.* **14**, 1 (2018).
- [15] G. M. Vanacore, G. Berruto, I. Madan, E. Pomarico, P. Biagioni, R. J. Lamb, D. McGrouther, O. Reinhardt, I. Kaminer, B. Barwick, H. Larocque, V. Grillo, E. Karimi, F. J. García de Abajo, and F. Carbone, Ultrafast generation and control of an electron vortex beam via chiral plasmonic near fields, *Nature Mater.* **18**, 573 (2019).
- [16] J. Verbeeck, H. Tian, and P. Schattschneider, Production and application of electron vortex beams, *Nature* **467**, 301 (2010).
- [17] A. Béché, R. Van Boxem, G. Van Tendeloo, and J. Verbeeck, Magnetic monopole field exposed by electrons, *Nature Phys.* **10**, 26 (2014).
- [18] V. Grillo, G. C. Gazzadi, E. Mafakheri, S. Frabboni, E. Karimi, and R. W. Boyd, Holographic Generation of Highly Twisted Electron Beams, *Phys. Rev. Lett.* **114**, 034801 (2015).
- [19] C. W. Clark, R. Barankov, M. G. Huber, M. Arif, D. G. Cory, and D. A. Pushin, Controlling neutron orbital angular momentum, *Nature* **525**, 504 (2015).
- [20] A. Luski, Y. Segev, R. David, O. Bitton, H. Nadler, A. R. Barnea, A. Gorchach, O. Cheshnovsky, I. Kaminer, and E. Narevicius, Vortex beams of atoms and molecules, *Science* **373**, 1105 (2021).
- [21] D. Sarenac, J. Nsofini, I. Hincks, M. Arif, C. W. Clark, D. G. Cory, M. G. Huber, and D. A. Pushin, Methods for preparation and detection of neutron spin-orbit states, *New J. Phys.* **20**, 103012 (2018).
- [22] D. Sarenac, C. Kapahi, W. Chen, C. W. Clark, D. G. Cory, M. G. Huber, I. Taminiou, K. Zhernenkov, and D. A. Pushin, Generation and detection of spin-orbit coupled neutron beams, *Proc. Natl. Acad. Sci.* **116**, 20328 (2019).
- [23] D. Sarenac, M. E. Henderson, H. Ekinici, C. W. Clark, D. G. Cory, L. Debeer-Schmitt, M. G. Huber, C. Kapahi, and D. A. Pushin, Experimental realization of neutron helical waves (2022), arXiv:2205.06263 [physics.app-ph].
- [24] A. J. Silenko, P. Zhang, and L. Zou, Manipulating Twisted Electron Beams, *Phys. Rev. Lett.* **119**, 243903 (2017).
- [25] A. J. Silenko, P. Zhang, and L. Zou, Relativistic quantum dynamics of twisted electron beams in arbitrary electric and magnetic fields, *Phys. Rev. Lett.* **121**, 043202 (2018).
- [26] A. J. Silenko and O. V. Teryaev, Siberian snake-like behavior for an orbital polarization of a beam of twisted (vortex) electrons, *Phys. Part. Nucl. Lett.* **16**, 77 (2019).
- [27] U. D. Jentschura and V. G. Serbo, Generation of high-energy photons with large orbital angular momentum by Compton backscattering, *Phys. Rev. Lett.* **106**, 013001 (2011).
- [28] U. D. Jentschura and V. G. Serbo, Compton upconversion of twisted photons: backscattering of particles with non-planar wave functions, *Eur. Phys. J. C* **71**, 1 (2011).
- [29] I. P. Ivanov, Creation of two vortex-entangled beams in a vortex-beam collision with a plane wave, *Phys. Rev. A* **85**, 033813 (2012).
- [30] R. Van Boxem, B. Partoens, and J. Verbeeck, Inelastic electron-vortex-beam scattering, *Phys. Rev. A* **91**, 032703 (2015).
- [31] D. V. Karlovets, S. S. Baturin, G. Geloni, G. K. Szykh, and V. G. Serbo, Generation of vortex particles via generalized measurements, *Eur. Phys. J. C* **82**, 1008 (2022).
- [32] D. V. Karlovets, S. S. Baturin, G. Geloni, G. K. Szykh, and V. G. Serbo, Shifting physics of vortex particles to higher energies via quantum entanglement, *Eur. Phys. J. C* **83**, 372 (2023).
- [33] S. Barnett, *Quantum Information* (Oxford University Press, 2009).
- [34] M. A. Al Khafaji, C. M. Cisowski, H. Jimbrow, S. Croke, S. Pádua, and S. Franke-Arnold, Single-shot characterization of vector beams by generalized measurements, *Optics Express* **30**, 22396 (2022).
- [35] G. Breit and J. A. Wheeler, Collision of two light quanta, *Phys. Rev.* **46**, 1087 (1934).
- [36] H. Bethe and W. Heitler, On the Stopping of fast particles and on the creation of positive electrons, *Proc. Roy. Soc. Lond. A* **146**, 83 (1934).
- [37] J. W. Motz, H. A. Olsen, and H. W. Koch, Pair production by photons, *Rev. Mod. Phys.* **41**, 581 (1969).
- [38] Y.-S. Tsai, Pair Production and Bremsstrahlung of Charged Leptons, *Rev. Mod. Phys.* **46**, 815 (1974), [Erratum: *Rev. Mod. Phys.* **49**, 421–423 (1977)].
- [39] S. R. Klein,  $e^+e^-$  pair production from 10-GeV to 10-ZeV, *Radiat. Phys. Chem.* **75**, 696 (2006).
- [40] M. Aaboud *et al.* (ATLAS), Evidence for light-by-light scattering in heavy-ion collisions with the ATLAS detector at the LHC, *Nature Phys.* **13**, 852 (2017).
- [41] J. Adam *et al.* (STAR), Measurement of  $e^+e^-$  Momentum and Angular Distributions from Linearly Polarized Photon Collisions, *Phys. Rev. Lett.* **127**, 052302 (2021).
- [42] J. D. Brandenburg, J. Seger, Z. Xu, and W. Zha, Report on progress in physics: observation of the Breit–Wheeler process and vacuum birefringence in heavy-ion collisions, *Rept. Prog. Phys.* **86**, 083901 (2023).
- [43] S. Weber *et al.*, P3: An installation for high-energy density plasma physics and ultra-high intensity laser–matter interaction at ELI-Beamlines, *Matter Radiat. Extremes* **2**, 149 (2017).
- [44] E. Carlidge, The light fantastic, *Science* **359**, 382 (2018).
- [45] C. N. Danson, C. Haefner, and J. Bromage *et al.*, Petawatt and exawatt class lasers worldwide, *High Power Laser Sci. Eng.* **7**, e54 (2019).
- [46] J. W. Yoon, C. Jeon, and J. Shin *et al.*, Achieving the laser intensity of  $5.5 \times 10^{22}$  W/cm<sup>2</sup> with a wavefront-corrected multi-PW laser, *Opt. Express* **27**, 20412 (2019).
- [47] J. W. Yoon, Y. G. Kim, I. W. Choi, J. H. Sung, H. W. Lee, S. K. Lee, and C. H. Nam, Realization of laser intensity over  $10^{23}$  W/cm<sup>2</sup>, *Optica* **8**, 630 (2021).
- [48] A. Di Piazza, C. Müller, K. Z. Hatsagortsyan, and C. H. Keitel, Extremely high-intensity laser interactions with fundamental quantum systems, *Rev. Mod. Phys.* **84**, 1177 (2012).
- [49] A. Gonoskov, T. G. Blackburn, M. Marklund, and S. S. Bulanov, Charged particle motion and radiation in strong electromagnetic fields, *Rev. Mod. Phys.* **94**, 045001 (2022).
- [50] A. Fedotov, A. Ilderton, F. Karbstein, B. King, D. Seipt, H. Taya, and G. Torgrimsson, Advances in QED with intense background fields, *Phys. Rept.* **1010**, 1 (2023).
- [51] S. S. Bulanov, C. Benedetti, D. Terzani, C. B. Schroeder, E. Esarey, T. Blackburn, and M. Marklund, A high-intensity laser-based positron source, (2023), arXiv:2311.10836 [physics.plasm-ph].
- [52] M. Vranic, O. Klimo, G. Korn, and S. Weber, Multi-GeV electron-positron beam generation from laser-electron scattering, *Sci. Rep.* **8**, 4702 (2018).
- [53] Y.-Y. Chen, P.-L. He, R. Shaisultanov, K. Z. Hatsagortsyan, and C. H. Keitel, Polarized positron beams via intense two-color laser pulses, *Phys. Rev. Lett.* **123**, 174801 (2019).
- [54] F. Wan, R. Shaisultanov, Y.-F. Li, K. Z. Hatsagortsyan, C. H. Keitel, and J.-X. Li, Ultrarelativistic polarized positron jets via collision of electron and ultraintense laser beams, *Phys. Lett. B* **800**, 135120 (2020).
- [55] Y.-F. Li, Y.-Y. Chen, W.-M. Wang, and H.-S. Hu, Production of Highly Polarized Positron Beams via Helicity Transfer from Polarized Electrons in a Strong Laser Field, *Phys. Rev. Lett.* **125**, 044802 (2020).

- [56] M. Büscher, A. Hützen, L. Ji, and A. Lehrach, Generation of polarized particle beams at relativistic laser intensities, *High Power Laser Sci. Eng.* **8**, e36 (2020).
- [57] H.-H. Song, W.-M. Wang, and Y.-T. Li, Dense Polarized Positrons from Laser-Irradiated Foil Targets in the QED Regime, *Phys. Rev. Lett.* **129**, 035001 (2022).
- [58] Y.-N. Dai, B.-F. Shen, J.-X. Li, R. Shaisultanov, K. Z. Hatsagortsyan, C. H. Keitel, and Y.-Y. Chen, Photon polarization effects in polarized electron–positron pair production in a strong laser field, *Matter Radiat. Extremes* **7**, 014401 (2022).
- [59] T. Sun, Q. Zhao, K. Xue, Z.-W. Lu, L.-L. Ji, F. Wan, Y. Wang, Y. I. Salamin, and J.-X. Li, Production of polarized particle beams via ultraintense laser pulses, *Rev. Mod. Plasma Phys.* **6**, 38 (2022).
- [60] K. Xue, T. Sun, K.-J. Wei, Z.-P. Li, Q. Zhao, F. Wan, C. Lv, Y.-T. Zhao, Z.-F. Xu, and J.-X. Li, Generation of High-Density High-Polarization Positrons via Single-Shot Strong Laser-Foil Interaction, *Phys. Rev. Lett.* **131**, 175101 (2023).
- [61] D. Y. Ivanov, G. L. Kotkin, and V. G. Serbo, Complete description of polarization effects in e+e- pair production by a photon in the field of a strong laser wave, *Eur. Phys. J. C* **40**, 27 (2005).
- [62] J. R. Danielson, D. H. E. Dubin, R. G. Greaves, and C. M. Surko, Plasma and trap-based techniques for science with positrons, *Rev. Mod. Phys.* **87**, 247 (2015).
- [63] M. J. A. Jansen, J. Z. Kamiński, K. Krajewska, and C. Müller, Strong-field Breit-Wheeler pair production in short laser pulses: Relevance of spin effects, *Phys. Rev. D* **94**, 013010 (2016).
- [64] D. Seipt and B. King, Spin- and polarization-dependent locally-constant-field-approximation rates for nonlinear Compton and Breit-Wheeler processes, *Phys. Rev. A* **102**, 052805 (2020).
- [65] G. Torgrimsson, Loops and polarization in strong-field QED, *New J. Phys.* **23**, 065001 (2021).
- [66] Y.-Y. Chen, K. Z. Hatsagortsyan, C. H. Keitel, and R. Shaisultanov, Electron spin- and photon polarization-resolved probabilities of strong-field QED processes, *Phys. Rev. D* **105**, 116013 (2022).
- [67] S. Tang, Fully polarized nonlinear Breit-Wheeler pair production in pulsed plane waves, *Phys. Rev. D* **105**, 056018 (2022).
- [68] K.-H. Zhuang, Y.-Y. Chen, Y.-F. Li, K. Z. Hatsagortsyan, and C. H. Keitel, Laser-driven lepton polarization in the quantum radiation-dominated reflection regime, *Phys. Rev. D* **108**, 033001 (2023).
- [69] Y.-Y. Chen, J.-X. Li, K. Z. Hatsagortsyan, and C. H. Keitel,  $\gamma$ -Ray Beams with Large Orbital Angular Momentum via Nonlinear Compton Scattering with Radiation Reaction, *Phys. Rev. Lett.* **121**, 074801 (2018).
- [70] X.-L. Zhu, T.-P. Yu, M. Chen, S.-M. Weng, and Z.-M. Sheng, Generation of GeV positron and  $\gamma$ -photon beams with controllable angular momentum by intense lasers, *New J. Phys.* **20**, 083013 (2018).
- [71] J. Zhao, Y.-T. Hu, Y. Lu, H. Zhang, L.-X. Hu, X.-L. Zhu, Z.-M. Sheng, I. C. E. Turcu, A. Pukhov, F.-Q. Shao, and T.-P. Yu, All-optical quasi-monoenergetic GeV positron bunch generation by twisted laser fields, *Commun. Phys.* **5**, 15 (2022).
- [72] C.-W. Zhang, D.-S. Zhang, and B.-S. Xie, Generation of  $\gamma$ -photons and pairs with transverse orbital angular momentum via spatiotemporal optical vortex pulse, (2024), arXiv:2403.16414 [physics.optics].
- [73] V. I. Ritus, Quantum effects of the interaction of elementary particles with an intense electromagnetic field, *J. Russ. Laser Res.* **6**, 497 (1985).
- [74] See Supplemental Materials for details on the theoretical framework and numerical results for the NBW scattering of vortex  $\gamma$  photons in CP lasers.
- [75] K. Y. Bliokh, M. R. Dennis, and F. Nori, Relativistic Electron Vortex Beams: Angular Momentum and Spin-Orbit Interaction, *Phys. Rev. Lett.* **107**, 174802 (2011).
- [76] E. Leader, The photon angular momentum controversy: Resolution of a conflict between laser optics and particle physics, *Phys. Lett. B* **756**, 303 (2016).
- [77] S. Lei, Z. Bu, W. Wang, B. Shen, and L. Ji, Generation of relativistic positrons carrying intrinsic orbital angular momentum, *Phys. Rev. D* **104**, 076025 (2021).
- [78] S. Lei, S. Liu, W. Wang, Z. Bu, B. Shen, and L. Ji, Transfer of spin to orbital angular momentum in the Bethe-Heitler process, *Phys. Rev. D* **108**, 036001 (2023).
- [79] Y. Taira, T. Hayakawa, and M. Katoh, Gamma-ray vortices from nonlinear inverse Thomson scattering of circularly polarized light, *Sci. Rep.* **7**, 1 (2017).
- [80] O. V. Bogdanov, P. Kazinski, and G. Y. Lazarenko, Semiclassical probability of radiation of twisted photons in the ultrarelativistic limit, *Phys. Rev. D* **99**, 116016 (2019).
- [81] M. Ababekri, R.-T. Guo, F. Wan, B. Qiao, Z. Li, C. Lv, B. Zhang, W. Zhou, Y. Gu, and J.-X. Li, Vortex  $\gamma$  photon generation via spin-to-orbital angular momentum transfer in nonlinear Compton scattering, *Phys. Rev. D* **109**, 016005 (2024).
- [82] R.-T. Guo, M. Ababekri, Q. Zhao, Y. I. Salamin, L.-L. Ji, Z.-G. Bu, Z.-F. Xu, X.-F. Weng, and J.-X. Li, Generation of  $\gamma$  photons with extremely large orbital angular momenta, (2023), arXiv:2310.16306 [hep-ph].
- [83] D. L. Burke *et al.*, Positron production in multi-photon light by light scattering, *Phys. Rev. Lett.* **79**, 1626 (1997).
- [84] H. Hu, C. Muller, and C. H. Keitel, Complete QED theory of multiphoton trident pair production in strong laser fields, *Phys. Rev. Lett.* **105**, 080401 (2010).
- [85] A. J. Macleod (LUXE), From theory to precision modelling of strong-field QED in the transition regime, *J. Phys. Conf. Ser.* **2249**, 012022 (2022).
- [86] F. C. Salgado *et al.*, Single particle detection system for strong-field QED experiments, *New J. Phys.* **24**, 015002 (2022).
- [87] H. Abramowicz *et al.*, Conceptual design report for the LUXE experiment, *Eur. Phys. J. ST* **230**, 2445 (2021).
- [88] V. N. Baier, V. M. Katkov, and V. M. Strakhovenko, *Electromagnetic processes at high energies in oriented single crystals* (1998).